Inorg. Chem. **2007**, *46*, 2563–2570

Inorganic Chemistry
Article

Syntheses and Characterizations of Palladium-Based Molecular Triangle/Square Compounds and Hybrid Composites with Polyoxometalates

Kazuhiro Uehara,[†] **Ko Kasai,**[‡] **and Noritaka Mizuno***[,†,‡]

Department of Applied Chemistry, School of Engineering, The University of Tokyo, 7-3-1 Hongo, Bunkyo-ku, Tokyo 113-8656, Japan, and Core Research for Evolutional Science and Technology (CREST), Japan Science and Technology Agency (JST), 4-1-8 Honcho, Kawaguchi, Saitama 332-0012, Japan

Received November 13, 2006

Syntheses and characterizations of a Pd-based molecular triangle and square and hybrid composites with polyoxometalates are examined. The equilibrium between the Pd-based molecular triangle $[(en^*)Pd(4,4'\text{-bpy})]_3(NO_3)_6$ and square $[(en^*)Pd(4,4'\text{-bpy})]_4(NO_3)_8$ largely depends on the solvents, and both compounds have successfully been isolated: $[(en^*)Pd(4,4'\text{-bpy})]_3(NO_3)_6 \cdot 3.5DMSO$, monoclinic *Cc* (No. 9), $a = 19.8210(2)$ Å, $b = 34.3667(5)$ Å, $c = 27.5484(4)$ Å, $\beta = 89.9420(10)°$, $V = 18765.5(4)$ Å^3; $[(en^*)Pd(4,4'\text{-bpy})]_4(NO_3)_8$, monoclinic *C*2/c (No. 15), $a = 45.6921(16)$ Å, $b = 8.7721(8)$ Å, $c = 36.719(3)$ Å, $\beta = 126.509(2)°$, $V = 11829.4(14)$ Å^3. The reactions of the Pd-based molecular triangle/square with $[W_6O_{19}]^{2-}$, $[W_{10}O_{32}]^{4-}$, and $[\alpha\text{-}SiW_{12}O_{40}]^{4-}$ form $\{[(en^*)Pd(4,4'\text{-bpy})]_4[\supset W_6O_{19}]\}[W_6O_{19}]_3$, $\{[(en^*)Pd(4,4'\text{-bpy})]_4[\supset W_6O_{19}]\}(NO_3)_6$, $\{[(en^*)Pd(4,4'\text{-bpy})]_4[\supset W_{10}O_{32}]\}[W_{10}O_{32}]$, $[(en^*)Pd(4,4'\text{-bpy})]_4[W_{10}O_{32}]_2$, and $[(en^*)Pd(4,4'\text{-bpy})]_4[\alpha\text{-}SiW_{12}O_{40}]_2$. The molecular square does not encapsulate the largest $[\alpha\text{-}SiW_{12}O_{40}]^{4-}$, but it does encapsulate $[W_6O_{19}]^{2-}$ and $[W_{10}O_{32}]^{4-}$. The isolation of $[W_6O_{19}]^{2-}$ and $[\alpha\text{-}SiW_{12}O_{40}]^{4-}$ from the mixture by use of the molecular square is possible by utilizing the quite different solubility of $\{[(en^*)Pd(4,4'\text{-bpy})]_4[\supset W_6O_{19}]\}(NO_3)_6$ and $[(en^*)Pd(4,4'\text{-bpy})]_4[\alpha\text{-}SiW_{12}O_{40}]_2$ formed in DMSO. The size-selective encapsulation property of supramolecules may open the new way to rationalize isolation methods of the useful polyoxometalates.

Introduction

The design of supramolecules has attracted much attention because they can be utilized for the molecular recognition, separation, gas storage, etc.[1] In particular, the molecular square is one of the simplest self-assemblies exhibiting such properties.[2−5] The molecular squares exhibit (i) the molecular triangle to square equilibrium and (ii) the molecular recognition of hydrophobic organic molecules.[4] The isolated, structurally characterized Pd-based molecular triangle is previously unknown, while there are two examples of isolated, structurally characterized Pt-based molecular triangles.[5a,b] In a series of ionic supramolecular compounds, −1-charged anions such as NO_3^-, PF_6^-, and OTf^- are usually

---

* To whom correspondence should be addressed. E-mail: tmizuno@mail.ecc.u-tokyo.ac.jp.

[†] Japan Science and Technology Agency (JST).

[‡] The University of Tokyo.

(1) (a) Lehn, J.-M. *Supramolecular Chemistry*; VCH: Weinheim, Germany, 1995. (b) *Supramolecular Organometallic Chemistry*; Haiduc, I., Edelmann, F. T., Eds.; VCH: Weinheim, Germany, 1999.

(2) (a) Stang, P. J.; Olenyuk, B. *Acc. Chem. Res.* 1**997**, *30*, 502. (b) Fujita, M.; Tominaga, M.; Hori, A.; Therrien, B. *Acc. Chem. Res.* **2005**, *35*, 371. (c) Leininger, S.; Olenyuk, B.; Stang, P. J. *Chem. Rev.* **2000**, *100*, 853. (d) Amijs, C. H. M.; van Klink, G. P. M.; van Koten, G. *J. Chem. Soc., Dalton Trans*. **2006**, 308.

(3) Molecular triangle and square based on the octahedral vertices: (a) Cotton, F. A.; Lin, C.; Murillo, C. A. *Acc. Chem. Res.* **2001**, *34*, 759. (b) Cotton, F. A.; Daniels, L. M.; Lin, C.; Murillo, C. A. *J. Am. Chem. Soc.* **1999**, *121*, 4538. (c) Cotton, F. A.; Lin, C.; Murillo, C. A. *Inorg. Chem.* **2001**, *40*, 575. (d) Cotton, F. A.; Murillo, C. A.; Yu, R. *J. Chem. Soc., Dalton Trans.* **2006**, 3900. (e) Cotton, F. A.; Liu, C. Y.; Murillo, C. A.; Wang, X. *Inorg. Chem.* **2006**, *45*, 2619. (f) Angaridis, P.; Berry, J. F.; Cotton, F. A.; Murillo, C. A.; Wang, X. *J. Am. Chem. Soc.* **2003**, *125*, 10327. (g) Cotton, F. A.; Murillo, C. A.; Wang, X.; Yu, R. *Inorg. Chem.* **2004**, *43*, 2004.

(4) Molecular recognition by molecular squares: (a) Fujita, M.; Yazaki, J.; Ogura, K. *Tetrahedron Lett.* **1991**, *32*, 5589. (b) Lee, S. B.; Hwang, S.; Chung, D. S.; Yun, H.; Hong, J.-I. *Tetrahedron Lett.* **1998**, *39*, 873. (c) Willemann, M.; Mulcahy, C.; Sigel, R. K. O.; Cerdá, M. M.; Freisinger, E.; Miguel, P. J. S.; Roitzsch, M.; Lippert, B. *Inorg. Chem.* **2006**, *45*, 2093.

(5) (a) Schweiger, M.; Seidel, S. R.; Arif, A. M.; Stang, P. J. *Inorg. Chem.* **2002**, *41*, 2556. (b) Schweiger, S.; Seidel, S. R.; Arif, A. M.; Stang, P. J. *Angew. Chem., Int. Ed.* **2001**, *40*, 3467. (c) Schnebeck, R.-D.; Freisinger, E. Glahé, F.; Lippert, B. *J. Am. Chem. Soc.* **2000**, *122*, 1381. (d) Lai, S.-W.; Chan, M. C.-W.; Peng, S.-M.; Che, C.-M. *Angew. Chem., Int. Ed.* **1999**, *38*, 669. (e) Fujita, M.; Sasaki, O.; Mitsuhashi, T.; Fujita, T.; Yazaki, J.; Yamaguchi, K.; Ogura, K. *J. Chem. Soc., Chem. Commun.* **1996**, 1553. (f) Ferrer, M.; Mounir, M.; Rossell, O.; Ruiz, E.; Maestro, M. A. *Inorg. Chem.* **2003**, *42*, 5890.

10.1021/ic062156r CCC: $37.00

used as counteranions. Therefore, the influence of large, highly negatively charged anions on the resulting supramolecular structure remained to be explored.[6]

Polyoxometalates (POMs) are oxide cluster anions with discrete structures. Much attention has been paid to the chemistry of POMs, because POMs work as catalysts, sorbents, electronic materials, medicine, etc., and the properties can be controlled at atomic/molecular levels.[7] While supramolecular POMs[8] or POM derivatives functionalized by the introduction of cationic organometallic fragments[9,10] have extensively been studied, little is known about the rational encapsulation of POMs by the organometallic frameworks.[10] The size-selective encapsulation property of supramolecules may open the new way to rationalize the isolation methods of the useful polyoxometalates. We have also reported the layered coordination polymer consisting of the Keggin-type polyoxometalate and (ethylenediamine)palladium complex fragment, $\{[(\mathrm{en})\mathrm{Pd}(4,4\text{-bpy})]_2[\alpha\text{-}\mathrm{SiW}_{12}\mathrm{O}_{40}]\}_\infty$.[11] The palladium complex fragment does not form the putative molecular square in this system, probably because of (i) the presence of the large, highly negatively charged Keggin-type POM and (ii) the stabilization of the layered structure by the hydrophilic interaction between the layers.

In this article, we report syntheses and characterizations of (i) the Pd-based molecular triangle and square $[(\mathrm{en}^*)\mathrm{Pd}(4,4'\text{-bpy})]_n(\mathrm{NO}_3)_{2n}$ (en*, *N*,*N*,*N*′,*N*′-tetramethylethylenediamine; $n = 3$ (**1a**), 4 (**1b**)) and (ii) the hybrid composites with POMs, $\{[(\mathrm{en}^*)\mathrm{Pd}(4,4'\text{-bpy})]_4[\supset\mathrm{W}_6\mathrm{O}_{19}]\}[\mathrm{W}_6\mathrm{O}_{19}]_3$ (**2a**), $\{[(\mathrm{en}^*)\mathrm{Pd}(4,4'\text{-bpy})]_4[\supset\mathrm{W}_6\mathrm{O}_{19}]\}(\mathrm{NO}_3)_6$ (**2b**), $\{[(\mathrm{en}^*)\mathrm{Pd}(4,4'\text{-bpy})]_4[\supset\mathrm{W}_{10}\mathrm{O}_{32}]\}[\mathrm{W}_{10}\mathrm{O}_{32}]$ (**3a**), $[(\mathrm{en}^*)\mathrm{Pd}(4,4'\text{-bpy})]_4[\mathrm{W}_{10}\mathrm{O}_{32}]_2$ (**3b**), and $[(\mathrm{en}^*)\mathrm{Pd}(4,4'\text{-bpy})]_4[\alpha\text{-}\mathrm{SiW}_{12}\mathrm{O}_{40}]_2$ (**4**). The compounds **1a**,**b** mainly exist in DMSO and water, respectively. The molecular square does not encapsulate the Keggin POM in the cavity but does encapsulate $[\mathrm{W}_6\mathrm{O}_{19}]^{2-}$ and $[\mathrm{W}_{10}\mathrm{O}_{32}]^{4-}$. This property can be applied to the isolation of $[\mathrm{W}_6\mathrm{O}_{19}]^{2-}$ and $[\alpha\text{-}\mathrm{SiW}_{12}\mathrm{O}_{40}]^{4-}$ from the mixture.

Experimental Section

All procedures were carried out under aerobic conditions. Compounds $(\mathrm{en}^*)\mathrm{PdCl}_2$,[12] $(\mathrm{TBA})_2[\mathrm{W}_6\mathrm{O}_{19}]$,[13a] $(\mathrm{TBA})_4[\alpha\text{-}\mathrm{SiW}_{12}\mathrm{O}_{40}]$,[13b] and $(\mathrm{TBA})_4[\mathrm{W}_{10}\mathrm{O}_{32}]$[13c] were synthesized according to the published procedures. All reagents and solvents were used as purchased unless otherwise stated. ^{1}H, ^{13}C{H}, and ^{183}W NMR spectra were recorded on a JEOL EX-270 spectrometer equipped with Excalibur 6.0 for Windows. IR spectra were recorded on a JASCO FT-IR 580 spectrometer.

Diffraction measurements were made on a Rigaku Saturn 70 CCD area detector with Mo Kα radiation ($\lambda = 0.710\,69$ Å). The data collections were carried out at 153 K. Indexing was performed from 7 oscillation images, which were exposed for 5 s. The crystal-to-detector distance was 45 mm. Readout was performed with the pixel size of 70 × 70 mm. A total of 1080 images for each compounds were collected. A sweep of data was done using ω scans from -110 to 70° at $\kappa = 45°$ and $\phi = 0$, 70, and 140°. Neutral scattering factors were obtained from the standard source.[14] Data were corrected for Lorentz and polarization effects. Empirical absorption corrections were made with HKL 2000 for Linux.[15]

The molecular structures were solved by SHELX-97[16] linked to Win-GX for Windows.[17] As for **1a**, the molecular structure of **1a** could be solved only with the space group *Cc*. All the atoms of molecular triangle were refined anisotropically, and the nitrate anions and solvents of crystallization (DMSO) were refined isotropically. As for **1b**, all the atoms of molecular square were refined anisotropically and the nitrate anions were refined isotro-

---

[6] (a) Noro, S.; Kitaura, R.; Kondo, M.; Kitagawa, S.; Ishii, T.; Matsuzaka, H.; Yamashita, M. *J. Am. Chem. Soc.* **2002**, *124*, 2568. (c) Du, M.; Guo, Y.-M.; Chen, S.-T.; Bu, X.-H.; Batten, S. R.; Ribas, J.; Kitagawa, S. *Inorg. Chem.* **2004**, *43*, 1287. (d) Min, K. S.; Suh, M. P. *J. Am. Chem. Soc.* **2000**, *122*, 6834.

[7] (a) Okuhara, T.; Mizuno, N.; Misono, M. *Adv. Catal.* **1996**, *41*, 113. (b) Special issue on polyoxometalates: Hill, C. L., Ed. *Chem. Rev.* **1998**, *98*, 1. (c) *Polyoxometalate Chemistry for Nano-Composite Design*; Yamase, T., Pope, M. T., Eds.; Kluwer: Dordrecht, The Netherlands, 2002. (d) Kozhevnikov, I. V. In *Catalysis by Polyoxometalates*; Wiley: Chichester, U.K., 2002. (e) Pope M. T. In *Comprehensive Coordination Chemistry II*; Wedd, A. G., McCleverty, J. A., Meyer, T. J., Eds.; Elsevier: New York, 2004; Vol. 4, p 635. (f) Hill, C. L. In *Comprehensive Coordination Chemistry II*; Wedd, A. G., McCleverty, J. A., Meyer, T. J., Eds.; Elsevier: New York, 2004; Vol. 4, p 679. (g) Neumann R. In *Modern Oxidation Methods*; Bäckvall, J. E., Ed.; Wiley-VCH: Weinheim, Germany, 2004; p 223. (h) Mizuno, N.; Kamata, K.; Yamaguchi, K. In *Surface and Nanomolecular Catalysis*; Richards, R., Ed:, CRC Press: Boca Raton, FL, 2006; p 463.

[8] (a) Müller, A.; Reuter, H.; Dillinger, S. *Angew. Chem., Int. Ed.* **1995**, *34*, 2311. (b) Wassermann, K.; Dickman, M. H.; Pope, M. T. *Angew. Chem., Int. Ed.* **1997**, *36*, 1445. (c) Salignac, B.; Riedel, S.; Dolbecq, A.; Sécheresse, F.; Cadot, E. *J. Am. Chem. Soc.* **2000**, *122*, 10381. (d) Müller, A.; Bögge, E.; Schmidtmann, M.; Dress, A. *Angew. Chem., Int. Ed.* **2002**, *41*, 1162. (e) du Peloux, C.; Dolbecq, A.; Mialane, P.; Marrot, J.; Rivière, E.; Sécheresse, F. *Inorg. Chem.* **2002**, *41*, 7100. (f) Cadot, E.; Pouet, M.-J.; Robbert-Labarre, C.; de Peloux, C.; Marrot, J.; Sécheresse, F. *J. Am. Chem. Soc.* **2004**, *126*, 9127. (g) Mal, S. S.; Kortz, U. *Angew. Chem., Int. Ed.* **2005**, *44*, 3777. (h) Müller, A.; Todea, A. M.; van Slageren, J.; Dressel, M.; Bögge, H.; Schmidtmann, M.; Luban, M.; Engelhardt, L.; Rusu, M. *Angew. Chem., Int. Ed.* **2005**, *44*, 3857. (i) Müller, A.; Todea, A. M.; Bögge, H.; van Slageren, J.; Dressel, M.; Stammler, A.; Rusu, M. *Chem. Commun.* **2006**, 3066. (j) Long, D.-L.; Kögerler, P.; Parenty, A. D. C.; Fielden, J.; Cronin, L. *Angew. Chem., Int. Ed.* **2006**, *45*, 4798.

[9] (a) Gómez-García, C. J.; Ouahab, L.; Gimenez-Saiz, C.; Trinki, S.; Coronado, E.; Delhaés, P. *Angew. Chem., Int. Ed.* **1994**, *33*, 223. (b) Khan, M. I.; Yohannes, E.; Powell, D. *Inorg. Chem.* **1999**, *38*, 212. (c) Son, J. H.; Choi, H.; Kwon, Y. U. *J. Am. Chem. Soc.* **2000**, *122*, 7432. (d) Felices, L. S.; Vitoria, P.; Gutiérrez-Zorrilla, J. M.; Reinoso, S.; Etxebarria, J.; Lezama, L. *Chem.—Eur. J.* **2004**, *10*, 5138. (e) Ishii, Y.; Takenaka, Y.; Konishi, K. *Angew. Chem., Int. Ed.* **2004**, *43*, 2702. (f) Vasylyev, M. V.; Neumann, R. *J. Am. Chem. Soc.* **2004**, *126*, 884. (j) L.-Laronze, N.; Haouas, M.; Marrot, J.; Taulelle, F.; Hervé, G. *Angew. Chem., Int. Ed.* **2006**, *45*, 139. (k) An, H.-A.; Wang, E.-B.; Xiao, D.-R.; Li, Y.-G.; Su, Z.-M.; Xu, L. *Angew. Chem., Int. Ed.* **2006**, *45*, 904.

[10] The encapsulation of POMs by hydrothermal synthesis has been reported: (a) Hagrman, D.; Hagrman, P. J.; Zubieta, J. *Angew. Chem., Int. Ed.* **1999**, *38*, 2638. (b) Hagrman, P. J.; Hagrman, D.; Zubieta, J. *Angew. Chem., Int. Ed.* **1999**, *38*, 3165. (c) Férey, G.; Mellot-Draznieks, C.; Millange, F.; Dutour, J.; Surblé, S.; Margiolaki, I. *Science* **2005**, *39*, 2040. (d) Yang, L.; Naruke, H.; Yamase, T. *Inorg. Chem. Commun.* **2003**, *6*, 1020.

[11] Uehara, K.; Nakao, H.; Kawamoto, R.; Hikichi, S.; Mizuno, N. *Inorg. Chem.* **2006**, *45*, 9448.

[12] (a) Wojciechowski, W.; Matczak-jon, E. *Inorg. Chim. Acta* **1990**, *173*, 85. (b) Djuran, M. I.; Milinkovic, S. U. *Polyhedron* **2000**, *19*, 959.

[13] (a) Fournier, M. *Inorg. Synth.* **1990**, *27*, 80. (b) The tetrabutylammonium salt of $[\alpha\text{-}\mathrm{SiW}_{12}\mathrm{O}_{40}]$, $(\mathrm{TBA})_4[\alpha\text{-}\mathrm{SiW}_{12}\mathrm{O}_{40}]$, was synthesized by the addition of (TBA)Br to the aqueous solution of $\mathrm{K}_4[\alpha\text{-}\mathrm{SiW}_{12}\mathrm{O}_{40}]$: Tézé, A.; Hervé, G. *Inorg. Synth.* **1990**, *27*, 85. (c) Fournier, M. *Inorg. Synth.* **1990**, *27*, 81.

[14] *International Tables for X-ray Crystallography*; Kynoch Press: Birmingham, U.K., 1975; Vol. 4.

[15] Otwinowski, Z.; Minor, W. In *Processing of X-ray Diffraction Data Collected in Oscillation Mode, Methods in Enzimology, Macromolecular Crystallography, Part A*; Carter, C. W., Jr., Sweet, R. M., Eds.; Academic Press: New York, 1997; Vol. 276, p 307.

[16] Sheldrick, G. M. *SHELX-97, Programs for Crystal Structure Analysis*, release 97-2; University of Göttingen: Göttingen, Germany, 1997.

[17] Farrugia, L. J. *J. Appl. Crystallogr.* **1999**, *32*, 837.

pically. Hydrogen atoms of the molecular triangle and square were refined as riding models. As for **2a**,**b**, **3a**,**b**, and **4**, the heavy atoms (palladium and tungsten) were refined anisotropically and all the atoms except for the heavy atoms were refined isotropically.[18] Hydrogen atoms were not included for the structural solution. Since the structure of **3a** could not be obtained with the orthorhombic and monoclinic space groups, a lower symmetry of the triclinic space group was adopted. In the course of structural analysis, we met the difficulty that the thermal parameters of light atoms in part became almost zero or negative and the structure could not be solved. Therefore, a part of the isotropic thermal parameters was set to be equal (EADP in SHELX) as follows: The thermal parameters of the carbon and nitrogen atoms in *N*,*N*,*N*′,*N*′-tetramethylethylenediamine were set to be equal to one another, and those in 4,4′-bipyridine were set to be equal to one another. The thermal parameters of the oxygen atoms in decatungstate were also set to be equal to one another. The disordered atom combinations in **2b** were (C11A, C11B), (C12A, C12B), and (C13A, C13B) of the methyl groups in the *N*,*N*,*N*′,*N*′-tetramethylethylenediamine ligand coordinated to Pd1, (C22A, C22B) and (C23A, C23B) of those coordinated to Pd2, and (O902, O952), (S902, S922, S952), and (S903, S953) in DMSO solvents of crystallization. The respective occupancies were calculated to be (0.70, 0.30), (0.52, 0.48), (0.53, 0.47), (0.58, 0.42), (0.52, 0.48), (0.5, 0.5), (0.39, 0.25, 0.36), and (0.81, 0.19). The disordered atom combination in **3a** was (C36A, C36B) of the methylene group in the *N*,*N*,*N*′,*N*′-tetramethylethylenediamine ligand coordinated to Pd3, and the occupancy was calculated to be (0.61, 0.39). The disordered atom combinations in **4** were (C16A, C16B) of the methylene group in the *N*,*N*,*N*′,*N*′-tetramethylethylenediamine ligand coordinated to Pd1, (C35A, C35B, C36) of the methylene group in the *N*,*N*,*N*′,*N*′-tetramethylethylenediamine ligand coordinated to Pd3, and (S601, S651), (S602, S652), (S603, S653), and (S701, O701, C701, C702) in DMSO solvents of crystallization. The respective occupancies were calculated to be (0.39, 0.61), (0.85, 0.33, 0.82), (0.74, 0.26), (0.76, 0.24), (0.75, 0.25), and (0.5, 0.5, 0.5, 0.5). The positions of the disordered solvents of crystallization (acetone and water in **1a**, acetone and DMSO in **1b**, and DMSO in **3a**,**b**) were difficult to locate from the Fourier map and were squeezed by the use of the program PLATON.[19] These crystallographic data and the numbering schemes are depicted in Table 1 and Figures S3−S9, respectively.

CCDC 626149 (**1a**), 626150 (**1b**), 626151 (**2a**), 626152 (**2b**), 626153 (**3a**), 626154 (**3b**), and 626155 (**4**) contain the supplementary crystallographic data. These data can be obtained free of charge via www.ccdc.cam.ac.uk/conts/retrieving.html (or from the Cambridge Crystallographic Data Centre, 12 Union Road, Cambridge CB2 1EZ, U.K.; fax, (+44) 1223-336-033, or deposit@ccdc.cam.ac.uk).

Syntheses of $[(en^*)Pd(4,4'\text{-}bpy)]_3(NO_3)_6$ (1a) and $[(en^*)Pd(4,4'\text{-}bpy)]_4(NO_3)_8$ (1b). Treatment of (en*)PdCl$_2$ (0.300 g, 1.02 mmol) with AgNO$_3$ (0.347 g, 2.04 mmol) in H$_2$O immediately gave insoluble AgCl. The addition of 4,4′-bpy (0.160 g, 1.02 mmol) to the filtrate gave the yellow aqueous solution. The removal of H$_2$O by the evaporation gave the yellow solid. The single crystal of **1a** fit for the X-ray crystallography was obtained by the vapor diffusion of acetone into the DMSO solution of **1a** (0.260 g, 0.170 mmol, yield 50%). A single crystal of **1b** was obtained by the vapor diffusion of acetone into the H$_2$O solution of **1a**. IR (KBr, cm^{-1}): 3092 w, 3010 w, 2916 w, 1613 m, 1466 m, 1384 vs, 1222 w, 1103 w, 1044 m, 1023 m, 954 m, 825 m, 811 m, 769 s. ^{1}H NMR (270 MHz, DMSO-d_6, rt (room temperature)): δ_H (ppm) 9.33 (d, $^2J = 6.3$ Hz; Py(**1b**)), 9.18 (d, $^2J = 6.43$ Hz; Py(**1a**)), 8.21 (d, $^2J = 6.43$ Hz; Py(**1a**)), 8.14 (d, $^2J = 6.3$ Hz; Py(**1b**)), 2.96 (br s, CH$_2$), 2.59 (s, Me(**1a**)), 2.45 (s, Me(**1b**)). ^{13}C{H} NMR (67.8 MHz, DMSO-d_6, rt): δ_C (ppm) 151.78 (brs, Py(**1a** and **1b**)), 145.06 (ipso-Py-(**1a**)), 143.12 (ipso-Py(**1b**)), 124.66 (Py(**1b**)), 123.55 (Py(**1a**)), 62.26 (CH$_2$), 50.41 (Me(**1a**)), 50.15 (Me(**1b**)). Anal. Calcd for $N_{18}O_{28}S_7Pd_3C_{62}H_{120}$ (**1a**·7DMSO·3H$_2$O): C, 35.30; H, 5.73; N, 11.95; S, 10.64. Found: C, 35.05; H, 5.59; N, 11.69; S, 10.93.

Synthesis of $\{[(en^*)Pd(4,4'\text{-}bpy)]_4[\supset W_6O_{19}]\}[W_6O_{19}]_3$ (2a). Compound **1a** (0.0125 g, 8.06 μmol (6.21 μmol as **1b**)) and 4 equiv of (TBA)$_2$[W$_6$O$_{19}$] (0.0470 g, 24.8 μmol) were dissolved in 6 mL of DMSO. The vapor diffusion of acetone into the DMSO solution gave yellow crystals of **2a** (0.0296 g, 4.14 μmol) in 67% yield. Single crystals fit for the X-ray crystallography were obtained from DMF solution. IR (KBr, cm^{-1}): 3101 w, 3023 w, 2926 w, 1658 m, 1613 m, 1466 m, 1420 m, 1388 w, 977 s, 808 vs, 659 w, 587 m. ^{1}H NMR (270 MHz, DMSO-d_6, rt): δ_H (ppm) 9.19 (brs, 16H; Py), 8.23 (brs, 16H; Py), 2.95 (s, 16H), 2.72 (s, 48H; Me). ^{183}W NMR (11.2 MHz, DMSO-d_6, rt): δ_W (ppm) 58.84. Anal. Calcd for $N_{16}O_{80}S_4Pd_4W_{24}C_{72}H_{120}$ (**2a**·4DMSO): C, 11.60; H, 1.62; N, 3.01. Found: C, 11.46; H, 1.59; N, 3.34.

Synthesis of $\{[(en^*)Pd(4,4'\text{-}bpy)]_4[\supset W_6O_{19}]\}(NO_3)_6$ (2b). Compound **1a** (0.100 g, 66.3 μmol (48.4 μmol as **1b**)) and (TBA)$_2$[W$_6$O$_{19}$] (0.0820 g, 49.7 μmol) were dissolved in 3 mL of DMSO. The vapor diffusion of acetone into the DMSO solution gave yellow crystals of **2** (0.140 g, 30.3 μmol) in 61% yield. IR (KBr, cm^{-1}): 3100 w, 3012 m, 2917 w, 1614 s, 1537 w, 1469 m, 1384 vs, 1281 w, 1222 w, 1079 m, 1023 s, 971 s, 955 s, 810 vs, 771 m. ^{1}H NMR (270 MHz, DMSO-d_6, rt): δ_H (ppm) 9.18 (d, $^2J = 6.43$ Hz, 16H; Py), 8.27 (d, $^2J = 6.43$ Hz, 16H; Py), 2.94 (brs, 16H; CH$_2$), 2.43 (s, 48H; Me). ^{13}C{H} NMR (67.8 MHz, DMSO-d_6, rt): δ_C (ppm) 152.23, 144.73, 124.06 (Py), 61.97 (CH$_2$), 50.05 (Me). ^{183}W NMR (11.2 MHz, DMSO-d_6, rt): δ_W (ppm) 59.62. Anal. Calcd for $N_{22}O_{39}S_2Pd_4W_6C_{68}H_{108}$ (**2**·2DMSO): C, 23.67; H, 3.15; N, 8.93. Found: C, 23.58; H, 3.36; N, 8.81.

Syntheses of $\{[(en^*)Pd(4,4'\text{-}bpy)]_4[\supset W_{10}O_{32}]\}[W_{10}O_{32}]$ (3a) and $[(en^*)Pd(4,4'\text{-}bpy)]_4[W_{10}O_{32}]_2$ (3b). A DMSO (3 mL) solution of **1a** (0.0125 g, 8.29 μmol (6.21 μmol as **1b**)) was gently layered onto a DMSO solution (3 mL) of (TBA)$_4$[W$_{10}$O$_{32}$] (0.0413 g, 12.4 μmol). After the layer was allowed to stand for several days, a mixture of the pale yellow powders (0.0279 g, 4.49 μmol) was obtained in 72% yield. A mixture of the single crystals of **3a**,**b** fit for X-ray crystallography was obtained from the DMSO solution of **1a** and (TBA)$_4$[W$_{10}$O$_{32}$] (molar ratio = 1.33/1.00). IR (KBr, cm^{-1}): 3097 w, 3017 w, 2923 w, 1612 m, 1466 m, 1420 m, 1020 m, 957 s, 891 s, 799 vs, 657 m, 587 m. Anal. Calcd for $N_{16}O_{84}S_4Pd_4W_{20}C_{72}H_{152}$ (**3a**/**3b**·4DMSO·16H$_2$O): C, 12.69; H, 2.25; N, 3.29; S, 1.88. Found: C, 12.55; H, 2.00; N, 3.04; S, 2.20.

Synthesis of $[(en^*)Pd(4,4'\text{-}bpy)]_4[\alpha\text{-}SiW_{12}O_{40}]_2$ (4). A DMSO (3 mL) solution of **1a** (0.0250 g, 16.6 μmol) was gently layered

---

[18] The light atoms of the polyoxometalate derivatives could not often be refined anisotropically due to the existence of many heavy atoms. For example: (a) Sadakane, M.; Dickman, M. H.; Pope, M. T. *Inorg. Chem.* **2001**, *40*, 2751. (b) du Peloux, C.; Dolbecq, A.; Mialane, P.; Marrot, J.; Rivière, E.; Sécheresse, F. *Inorg. Chem.* **2002**, *41*, 7100. (c) Gaunt, A. J.; May, L.; Collison, D.; Fox, D. *Inorg. Chem.* **2003**, *42*, 5049. (d) Lei, C.; Mao, J.-G.; Sun, Y.-Q.; Song, J.-L. *Inorg. Chem.* **2004**, *43*, 1964. (e) Mazeaud, A.; Dromzee, Y.; Thouvenot, R. *Inorg. Chem.* **2000**, *39*, 4735. (f) Juraja, S.; Vu, T.; Richardt, P. J. S.; Bond, A. M.; Cardwell, T. J.; Cashion, J. D.; Fallon, G. D.; Lazarev, G.; Moubaraki, B.; Murray, K. S.; Wedd, A. G. *Inorg. Chem.* **2002**, *41*, 1072. (g) Dolbecq, A.; Cadot, E.; Eisner, D.; Sécheresse, F. *Inorg. Chem.* **1999**, *38*, 4217. (h) Villanneau, R.; Proust, A.; Robert, F.; Viellet, P.; Gouzerh, P. *Inorg. Chem.* **1999**, *38*, 4981. (i) Volkmer, D.; Bredenkötter, B.; Tellenbröker, J.; Kögerler, P.; Kurth, D. G.; Lehmann, P.; Schnablegger, H.; Schwahn, D.; Piepenbrink, M.; Krebs, B. *J. Am. Chem. Soc.* **2002**, *124*, 10489.

[19] van der Sluis, P.; Spek, L. *Acta Crystallogr.* **1990**, *A46*, 194.

Table 1. Crystallographic Data for **1a**,**b**, **2a**,**b**, **3a**,**b**, and **4**

param	**1a**·3.5DMSO	**1b**	**2a**·14DMF	**2b**·12DMSO
Empirical formula	$C_{110}H_{186}N_{36}Pd_6S_7O_{43}$	$C_{64}H_{96}N_{24}O_{24}Pd_4$	$C_{53}N_{15}O_{45}Pd_2W_{12}$	$C_{44}N_{11}O_{24.5}Pd_2S_6W_3$
fw	3563.77	2011.25	3985.68	2023.26
cryst system	monoclinic	monoclinic	triclinic	orthorhombic
lattice type	*C*-centered	*C*-centered	primitive	*C*-centered
space group	*Cc* (No. 9)	*C2/c* (No. 15)	$P\bar{1}$ (No. 2)	*Cmca* (No. 64)
lattice params (Å, deg)	$a = 19.8210(2)$	$a = 45.6921(16)$	$a = 11.5984(4)$	$a = 34.4639(8)$
	$b = 34.3667(5)$	$b = 8.7721(8)$	$b = 20.4269(7)$	$b = 29.9390(6)$
	$c = 27.5484(4)$	$c = 36.719(3)$	$c = 21.0980(10)$	$c = 15.0871(4)$
			$\alpha = 90.908(2)$	
	$\beta = 89.9420(10)$	$\beta = 126.509(2)$	$\beta = 103.321(2)$	
			$\gamma = 99.633(2)$	
V (Å^3)	18765.5(4)	11829.4(14)	4787.7(3)	15671.1(6)
Z value	4	4	2	8
d_{calcd} (g cm^{-3})	1.261	1.129	2.765	1.77
μ(Mo Kα) (cm^{-1})	71.1	65.9	148.00	51.01
no. of reflcns measd	25 308	14 980	24 173	10 154
no. of observns[a]	17 909	6012	14 585	4377
no. of variables	1389	444	575	176
R	0.0676	0.0870	0.0709	0.0864
R_w	0.2034	0.2531	0.2664	0.32

param	**3a**	**3b**	**4**·7.5DMSO
empirical formula	$C_{64}N_{16}O_{64}Pd_4W_{20}$	$C_{32}N_8O_{32}Pd_2W_{10}$	$C_{79}N_{16}O_{87.5}Pd_4S_{7.5}Si_2W_{24}$
fw	6119.4	3059.63	7683.53
cryst system	triclinic	triclinic	monoclinic
lattice type	primitive	primitive	primitive
space group	$P\bar{1}$ (No. 2)	$P\bar{1}$ (No. 2)	$P2_1/n$ (No. 14)
lattice params (Å, deg)	$a = 18.790(2)$	$a = 14.3773(8)$	$a = 20.4824(3)$
	$b = 20.633(3)$	$b = 16.9891(10)$	$b = 49.3372(8)$
	$c = 22.388(4)$	$c = 23.6467(17)$	$c = 27.4000(6)$
	$\alpha = 91.012(7)$	$\alpha = 73.883(3)$	
	$\beta = 92.822(10)$	$\beta = 89.413(2)$	$\beta = 109.0290(10)$
	$\gamma = 90.383(8)$	$\gamma = 72.568(4)$	
V (Å^3)	8668(2)	5277.3(6)	26175.8(8)
Z value	2	2	4
d_{calcd} (g cm^{-3})	2.345	1.956	1.992
μ(Mo Kα) (cm^{-1})	136.73	112.3	108.9
no. of reflcns measd	33 355	24 827	63 576
no. of observns[a]	4929	7410	18 469
no. of variables	570	349	1056
R	0.0973	0.0977	0.0784
R_w	0.2934	0.2733	0.2299

[a] Data with $F_o > 4.0\sigma(F_o)$.

onto a DMSO solution (3 mL) of $(TBA)_4[\alpha\text{-}SiW_{12}O_{40}]$ (0.0984 g, 25.6 μmol). After the layer was allowed to stand for several days, yellow crystals of **4** (0.0480 g, 6.70 μmol) fit for X-ray crystallography were obtained in 53% yield. IR (KBr, cm^{-1}): 3097 w, 3009 w, 2916 w, 1653 m, 1636 m, 1612 m, 1534 w, 1466 m, 1434 m, 1412 m, 1313 w, 1218 w, 1022 vs, 970 vs, 954 s, 920 vs, 885 s, 799 vs, 709 m, 533 m. Anal. Calcd for $N_{16}O_{93.5}S_{13.5}Pd_4W_{24}Si_2C_{91}H_{177}$ (**4**·13.5DMSO): C, 13.14; H, 2.14; N, 2.69; S, 5.20. Found: C, 13.58; H, 2.34; N, 2.90; S, 4.79.

Separation Experiment. Compound **1a** (66.3 μmol (49.7 μmol as **1b**)) was added to the DMSO/H_2O (2 mL/2 mL) solution (solution A). Separately, $(TBA)_2[W_6O_{19}]$ (11.5 μmol) and $(TBA)_4[\alpha\text{-}SiW_{12}O_{40}]$ (25.6 μmol) were added to the DMSO (2 mL) solution (solution B). To solution B, solution A was added, and the white-yellow crystalline solid **4** was successfully collected in almost quantitative yield (0.0910 g, 12.5 μmol, 98%). The white-yellow product was characterized by IR spectroscopy and X-ray crystallography. The addition of an excess amount of acetone to the filtrate gave white-yellow crystals **2b** (0.0206 g, 6.40 μmol, 55% isolated yield). The resultant product was characterized by IR, ^1H NMR, and X-ray crystallography.

Results and Discussion

Syntheses and Characterizations of the Molecular Triangle and Square. A novel Pd-based molecular triangle of **1a** was successfully synthesized by the reaction of (en*)-Pd$(NO_3)_2$ with 4,4′-bpy in H_2O (Scheme 1). The molecular structure of **1a** revealed the formation of molecular triangle, which was the first example of a structurally characterized Pd-based molecular triangle with a linear and long bridging ligand (Figure 1a and Tables 1, 2, and S1).[2] Compound **1a** was composed of two crystallographically independent molecules (A and B) with a *C*-centered monoclinic space group (Figure S3). The Pd···Pd distances, N(Py)−Pd−N(Py) angles, and torsion angles between 4,4′-bpy rings were close to each other (molecule A, Pd···Pd distances 11.0057(8)−11.0068(8) Å, N(Py)−Pd−N(Py) angles 85.2(3)−86.0(3)°, torsion angles between pyridyl rings 19.33−20.89°; molecule

Scheme 1

$$\text{(en*)PdCl}_2 \xrightarrow[\text{ii) 4,4'-bpy}]{\text{i) AgNO}_3} \left[\underset{\mathbf{1a}}{[\text{(en*)Pd(4,4'-bpy)}]_3(\text{NO}_3)_6} \rightleftharpoons \underset{\mathbf{1b}}{[\text{(en*)Pd(4,4'-bpy)}]_4(\text{NO}_3)_8} \right]$$

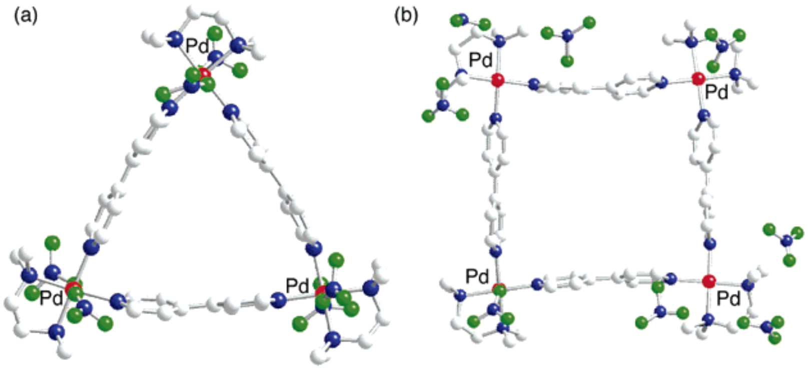

Figure 1. Ball and stick models of (a) **1a** and (b) **1b**.

Table 2. Selected Bond Distances and Angles for **1a**,**b**, **2a**,**b**, **3a**,**b,** and **4** (Distances in Å and Angles in deg)

	1a^{a}			
param	molecule A	molecule B	**1b**^{b}	**2a**^{b}
Pd−N(en*)	2.086(7), 2.072(7) 2.084(7), 2.033(8) 2.048(7), 2.071(8)	2.077(10), 2.046(8) 2.036(9), 2.86(9) 2.054(9), 2.022(9)	2.059(5), 2.062(7) 2.074(6), 2.084(6)	2.09(2), 2.101(16) 2.054(17), 2.089(17)
Pd−N(Py)	2.018(8), 2.059(7) 2.076(8), 2.010(7) 2.057(7), 2.040(8)	2.021(10), 2.021(8) 2.070(9), 2.024(9) 2.032(9), 2.033(8)	2.025(6), 2.024(6) 2.022(6), 2.047(6)	2.044(17), 2.042(17) 2.057(18), 2.000(17)
Pd···Pd(edge)	11.0057(8), 11.0068(8) 11.0059(8)	11.0095(9), 11.0114(8) 11.0069(8)	11.0624(21), 11.0898(6)	11.189(2), 11.119(2)
Pd···Pd(diagonal)			15.4080(8), 15.4733(10)	14.911(2), 16.5939(19)
N(en*)−Pd−N(en*)	85.8(3), 86.8(3) 84.8(3)	85.5(4), 85.5(4) 86.6(4)	85.0(2), 86.4(2)	84.5(7), 85.7(7)
N(en*)−Pd−N(Py)	94.2(3), 94.5(3) 93.2(3), 94.0(3) 95.9(3), 94.2(3)	93.0(4), 97.5(4) 93.6(4), 95.0(4) 94.3(4), 96.7(4)	95.1(2), 93.2(2) 92.4(2), 93.8(2)	90.4(7), 94.8(6) 90.2(7), 96.8(7)
N(Py)−Pd−N(Py)	85.6(3), 86.0(3) 85.2(3)	83.9(4), 86.0(4) 82.4(4)	86.8(2), 87.3(2)	90.3(7), 87.5(7)
torsion angle (4,4-bpy)	19.33, 20.15 20.89	17.49, 16.36 17.77	32.02, 21.89	4.61, 12.53

param	**2b**^{b}	**3a**	**3b**^{b}	**4**
Pd−N(en*)	2.046(13), 2.037(15)	2.06(4), 2.05(4) 2.125(19), 2.10(5) 2.09(4), 2.17(5) 2.19(5), 2.05(5)	2.06(2), 2.125(19) 2.11(3),2.07(2)	2.11(2), 2.18(2) 2.03(2), 2.15(2) 2.08(2), 2.23(2) 2.136(18), 2.09(2)
Pd−N(Py)	2.022(12), 2.017(12)	2.02(2), 2.02(2) 2.08(2), 2.06(3) 2.07(3), 2.05(3) 2.00(2), 2.02(2)	2.056(10), 2.049(11) 2.049(13), 2.026(11)	2.085(16), 2.05(2) 2.089(16), 2.041(17) 2.04(2), 2.06(2) 2.060(16), 2.046(17)
Pd···Pd(edge)	11.0846(15)	11.120(6), 11.163(5) 11.135(6), 11.114(5)	10.995(4), 11.084(3)	11.038(3), 11.074(2) 11.079(3). 11.027(2)
Pd···Pd(diagonal)	16.6047(19), 14.689(2)	15.670(5), 15.817(6)	16.751(3), 14.384(4)	12.666(2), 15.097(2)
N(en*)−Pd−N(en*)	86.1(7), 85.7(9)	87.8(11), 97.0(12) 83.4(14), 92.1(13)	84.9(9), 84.5(10)	87.6(9), 85.2(8) 92.7(8), 85.4(8)
N(en*)−Pd−N(Py)	93.0(5), 93.5(5)	95.6(14), 89.0(14) 86.4(15), 87.7(16) 95.4(16), 97.5(16) 90.2(16), 93.0(16)	96.1(8), 97.0(6) 93.8(9), 92.0(8)	89.1(8), 93.7(7) 94.0(7), 94.8(7) 94.1(7), 87.5(7) 94.0(6), 98.1(7)
N(Py)−Pd−N(Py)	87.9(7), 87.0(7)	87.8(11), 97.0(12) 83.4(14), 92.1(13)	82.1(6), 89.9(7)	89.6(6), 86.1(6) 85.8(7), 82.6(6)
torsion angle (4,4-bpy)	12.60, 12.83	8.389, 7.364 4.013, 0.557	21.68, 29.58	38.69, 40.89 34.92, 46.49

[a] The molecules A and B were crystallographically independent. [b] Sitting on a crystallographic mirror plane.

B, Pd···Pd distances 11.069(8)−11.0114(8) Å, N(Py)−Pd−N(Py) angles 82.4(4)−86.0(4)°, torsion angles between 4,4′-bpy rings 16.36−17.77°). The N(Py)−Pd−N(Py) angles and torsion angles between 4,4′-bpy rings deviated from the ideal angles of 60 and 0°, respectively. The +2 charge of Pd was compensated by two nitrate counteranions, which existed outside the cavity of the triangle.

The ^{1}H NMR spectrum of **1a** just after the dissolution in DMSO (<10 min) showed a set of bipyridyl signals: The intensities of signals at 9.18 and 8.14 ppm decreased with time, while a new set of signals appeared at 9.32 and 8.12 ppm with similar splitting patterns, which are attributable to the molecular triangle and square, respectively (Figure S1).[5e,f] The signal intensities almost unchanged after 24 h,

Scheme 2

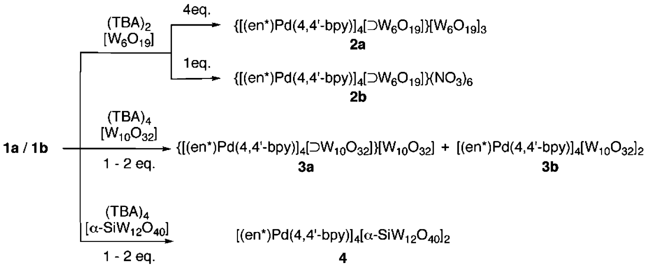

showing the achievement of the equilibrium between the molecular triangle and square. The equilibrium constant (K_{DMSO}) at 294 K was estimated to be $9.56 \pm 0.39\ \mathrm{M}^{-1}$.[20] On the other hand, the molecular square was a major species upon the dissolution of **1a** in D_2O, and the equilibrium constant (K_{water}) at 294 K was calculated to be $(2.48 \pm 0.02) \times 10^3\ \mathrm{M}^{-1}$ (Table S2 and Figure S2).

A single crystal of **1b** was successfully obtained by the vapor diffusion of acetone into the water solution. The X-ray analysis proved the formation of the molecular square of **1b** (Figure 1b and Tables 1, 2, and S1). The edge Pd···Pd distances (11.0624(21) and 11.0898(6) Å) and diagonal Pd···Pd distances (15.4080(8) and 15.4733(10) Å) reveal that the structure of **1b** is almost a regular square, while the N(Py)−Pd−N(Py) angles (86.8(2) and 87.3(2)°) and torsion angles of 4,4′-bpy rings (32.02 and 21.89°) deviated from the ideal angles of 90 and 0°. All the nitrate anions were outside of the cavity and neutralized the positive charge of ethylenediamine palladium moieties in the same way as those of **1a**.

Syntheses of Hybrid Composites between the Molecular Square and Polyoxometalate. We have recently reported the layered coordination polymer $\{[(\mathrm{en})\mathrm{Pd}(4,4'\text{-bpy})]_2[\alpha\text{-}\mathrm{SiW}_{12}\mathrm{O}_{40}]\}_\infty$ (en = ethylenediamine) with the hydrophilic guest sorption property between the layers.[11] The hydrogen-bonding affinity between the layers at the amine hydrogens of ethylenediamine ligand would be a key for the formation and stabilization of an unprecedented infinite chain structure. Therefore, we reached the idea that introduction of methyl substituents on the ethylenediamine ligand (the removal of hydrogen-bonding affinity) would lead to the formation of the hybrid composites with the molecular square moiety.

The hybrid composites of the molecular square and POMs were synthesized by the reaction of the molecular triangle/square (**1a**/**1b**) with $[\mathrm{W}_6\mathrm{O}_{19}]^{2-}$, $[\mathrm{W}_{10}\mathrm{O}_{32}]^{4-}$, and $[\alpha\text{-}\mathrm{SiW}_{12}\mathrm{O}_{40}]^{4-}$. The reaction of compound **1a**/**1b** with various amounts of TBA salts of POMs in DMSO resulted in the formation of the corresponding inorganic−organic hybrid composites, $\{[(\mathrm{en}^*)\mathrm{Pd}(4,4'\text{-bpy})]_4[\supset\mathrm{W}_6\mathrm{O}_{19}]\}[\mathrm{W}_6\mathrm{O}_{19}]$ (**2a**), $\{[(\mathrm{en}^*)\mathrm{Pd}(4,4'\text{-bpy})]_4[\supset\mathrm{W}_6\mathrm{O}_{19}]\}(\mathrm{NO}_3)_6$ (**2b**), a mixture of $\{[(\mathrm{en}^*)\mathrm{Pd}(4,4'\text{-bpy})]_4[\supset\mathrm{W}_{10}\mathrm{O}_{32}]\}[\mathrm{W}_{10}\mathrm{O}_{32}]$ (**3a**), and $[(\mathrm{en}^*)\mathrm{Pd}(4,4'\text{-bpy})]_4[\mathrm{W}_{10}\mathrm{O}_{32}]_2$ (**3b**), and $[(\mathrm{en}^*)\mathrm{Pd}(4,4'\text{-bpy})]_4[\alpha\text{-}\mathrm{SiW}_{12}\mathrm{O}_{40}]_2$ (**4**) in moderate yield (Scheme 2). The $[(\mathrm{en}^*)\mathrm{Pd}(4,4'\text{-bpy})]^{2+}$/POM ratios in **3a,b** and **4** were not changed by the molar ratios of the synthetic solutions, while the ratios in the products changed for the reaction with $(\mathrm{TBA})_2[\mathrm{W}_6\mathrm{O}_{19}]$.

The crystal structures of **2a,b**, **3a,b**, and **4** are shown in Figures 2−4 (see also Tables 1, 2, and S1). All compounds possessed the molecular square as a countercation. The edge distances (10.995(4)−11.189(2) Å) of the Pd square in compounds **2a,b**, **3a,b**, and **4** were very close to those in **1b**. The molecular square (13.8 Å × 12.3 Å) did not encapsulate the largest Keggin-type $[\alpha\text{-}\mathrm{SiW}_{12}\mathrm{O}_{40}]^{4-}$ (12.2 Å × 12.2 Å × 9.3 Å) in the cavity but only the Lindqvist-type hexatungstate (9.9 Å × 9.9 Å × 9.9 Å) and decatungstate (9.9 Å × 9.9 Å × 13.6 Å). Thus, the encapsulation of POMs with the molecular square depended on the sizes. There are several examples of the encapsulation of small, −1- or −2-charged anions by the supramolecules.[21] In addition, POMs encapsulated by the supramolecular frameworks have been synthesized with the starting reagents of POMs and supramolecular frameworks under hydrothermal conditions.[10] Therefore, the present rational encapsulation of large, −2- or −4-charged POMs with the supramolecules under milder conditions is still of importance.

The diagonal Pd···Pd distances in **2a** (16.5939(19) and 14.911(2) Å) and **2b** (16.6047(19) and 14.689(2) Å) were different from those of **1b** (15.4080(8) and 15.4733(10) Å), while those of **3a** (15.673(8) and 15.818(10) Å) were close to those of **1b**. The decatungstate $[\mathrm{W}_{10}\mathrm{O}_{32}]^{2-}$ was symmetrically encapsulated into the cavity of molecular square in **3a**, while the hexatungstate $[\mathrm{W}_6\mathrm{O}_{19}]^{2-}$ with the same diameter as that of $[\mathrm{W}_{10}\mathrm{O}_{32}]^{4-}$ was dissymmetrically encapsulated in **2a,b**. Such symmetry would influence the configuration of the Pd squares. The torsion angles of 4,4′-bpy rings in **2a,b** and **3a** (0.557−12.83°) were much smaller than those in **1b** (32.02 and 21.89°). This is probably because of the interaction between encapsulated POMs and 4,4′-bpy rings in **2a,b** and **3a**. The molecular square in **4** was much distorted (diagonal Pd···Pd distances, 15.10 and 12.67 Å; dihedral angles between two of the planes containing three palladium vertices, 67.11 and 49.02°), and such a molecular square has not yet been reported.

Upon the addition of **1a**/**1b** (3 equiv as **1b** with respect to **2a**) to the DMSO solution containing insoluble **2a**, DMSO soluble **2b** was formed in quantitative yield (Scheme 3), which was confirmed by IR, ^{1}H NMR, and X-ray crystallography (64% isolated yield). Thus, these $[\mathrm{W}_6\mathrm{O}_{19}]^{2-}$ Lindqvist-type POMs outside the cavity of $\{[(\mathrm{en}^*)\mathrm{Pd}(4,4'\text{-bpy})]_4\}^{8+}$ in **2a** could be encapsulated to form **2b**.

Compounds 2a,b in Solid and Solution States. The IR (KBr) measurements of **2a**,**b** were carried out to investigate the solid states. The IR spectrum of $(\mathrm{TBA})_2[\mathrm{W}_6\mathrm{O}_{19}]$ showed a $\nu(\mathrm{W{=}O})$ band at 975 cm^{-1}. On the other hand, the IR

---

[20] Since the solubility of compound **1a** in organic solvents was very low, the equilibrium constant in DMSO (K_{DMSO}) was measured at low concentration.

[21] Anion recognition by supramolecules. (a) ClO_4^-: Fujita, M.; Aoyagi, M.; Ogura, K. *Inorg. Chim. Acta.* **1996**, *246*, 53. (b) TfO$^-$, CuI_3^{2-}, ClO_4^-, and BF_4^-: Su, C.-Y.; Cai, Y.-P.; Chen, C.-L.; Smith, M. D.; Kaim, W.; zur Loye, H.-C. *J. Am. Chem. Soc.* **2003**, *125*, 8595. (c) $\mathrm{CF}_3\mathrm{SO}_3^-$, BF_4^-, and PF_6^-: Fochi, F.; Jacopozzi, P.; Wegelius, E.; Rissanen, K.; Cozzini, P.; Marastoni, E.; Fisicaro, E.; Manini, P.; Fokkens, R.; Dalcanale, E. *J. Am. Chem. Soc.* **2001**, *123*, 7539. (d) Kuehl, C. J.; Kryschenko, Y. K.; Radhakrishnon, U.; Seidel, S. R.; Huang, S. D.; Stang, P. J. *Proc. Natl. Acad. Sci. U.S.A.* **2002**, *99*, 4932.

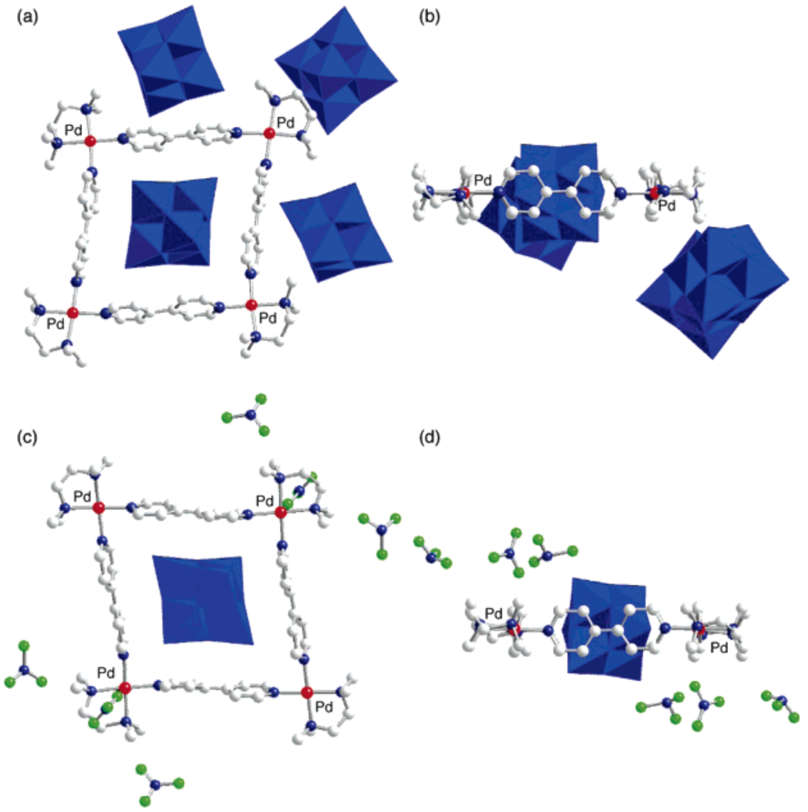

Figure 2. Molecular structures of **2a**,**b**: Top and side views of **2a** (a and b) and top and side views of **2b** (c and d). The molecular square is depicted with the ball and stick model, and $[W_6O_{19}]^{2-}$ is depicted with the polyhedra representation.

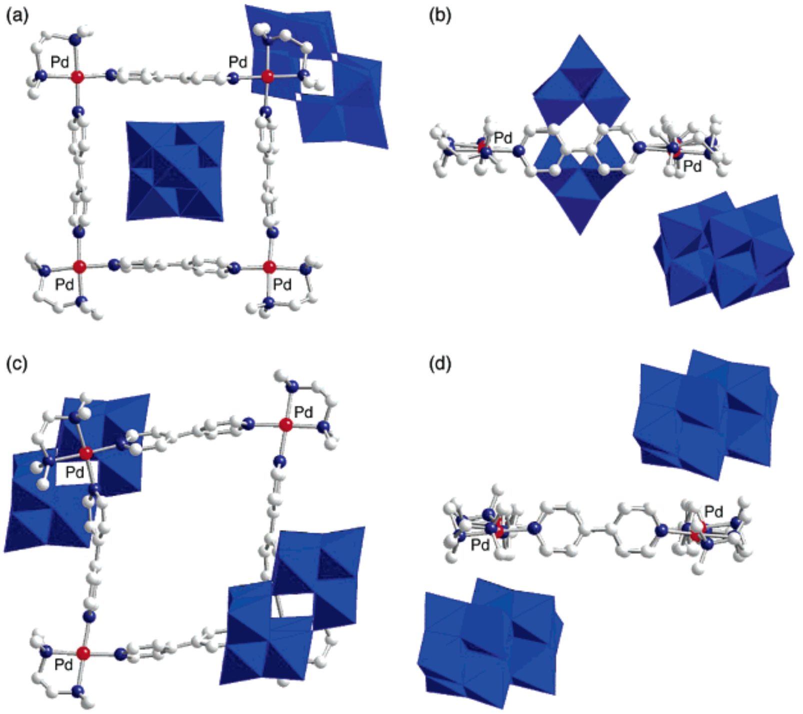

Figure 3. Molecular structures of **3a**,**b**: Top and side views of **3a** (a and b) and top and side views of **3b** (c and d). The molecular square is depicted with the ball and stick model, and $[W_{10}O_{32}]^{4-}$ is depicted in the polyhedra representation.

spectra of **2a**,**b** showed two bands at 977 s and 957 sh cm^{-1} and 971 s and 955 w cm^{-1}, respectively. The appearance of the 955−957 cm^{-1} band would result from the interaction between the molecular square and hexatungstate. Next, the NMR measurements of compounds **2a**,**b** in DMSO-d_6 were carried out to investigate the solution states, since compounds **3a**,**b** and **4** were almost insoluble in any solvents. The ^{1}H NMR spectrum of **2a** (**2b**) in DMSO-d_6 also gave a single set of signals at 9.19 (9.18) and 8.23 (8.27) ppm assignable to the 4,4′-bipyridine ligand of the molecular square, and

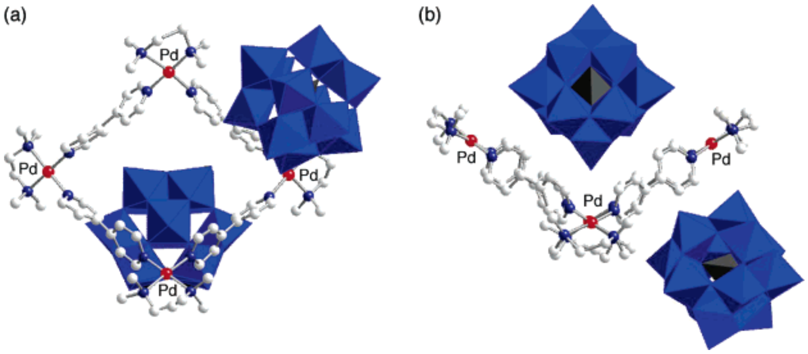

Figure 4. Molecular structure of **4**: (a) top and (b) side views. The molecular square is depicted with the ball and stick model, and $[\alpha\text{-SiW}_{12}O_{40}]^{4-}$ is depicted in the polyhedra representation.

Scheme 3

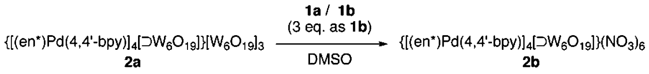

$$\underset{\mathbf{2a}}{\{[(en^*)Pd(4,4'\text{-bpy})]_4[\supset W_6O_{19}]\}[W_6O_{19}]_3} \xrightarrow[\text{DMSO}]{\mathbf{1a}\,/\,\mathbf{1b}\ (3\text{ eq. as }\mathbf{1b})} \underset{\mathbf{2b}}{\{[(en^*)Pd(4,4'\text{-bpy})]_4[\supset W_6O_{19}]\}(NO_3)_6}$$

Scheme 4

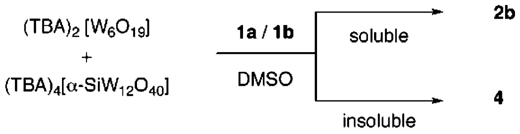

the signal positions were different from the 9.33 and 8.14 ppm of **1b**. The ^{183}W NMR spectra of **2a**,**b** exhibited single signals at 58.84 and 59.62 ppm, respectively, which appeared at lower fields than that of $(TBA)_2[W_6O_{19}]$ (58.14 ppm). These ^{1}H and ^{183}W NMR shifts would result from the interaction between the molecular square and hexatungstate in the solution state. The fact that **2a** (**2b**) showed a single ^{183}W NMR signal suggests the rapid exchange between the hexatungstates inside and outside the cavity of the molecular square in **2a** (**2b**).

Separation Experiment with 1. Generally, a separation of oxide cluster such as POMs is quite difficult by the conventional method. The size-selective encapsulation property of supramolecule may open a new way to rationalize isolation methods of the useful polyoxometalates. So we examined the separation experiment for the mixture of $[W_6O_{19}]^{2-}$ and $[\alpha\text{-SiW}_{12}O_{40}]^{4-}$ with **1**. Compound **2b** was soluble in DMSO, while compound **4** was insoluble. This property could be applied to the separation of $[W_6O_{19}]^{2-}$ and $[\alpha\text{-SiW}_{12}O_{40}]^{4-}$ POMs (Scheme 4). Compound **1a** (66.3 μmol (49.7 μmol as **1b**)) was added to DMSO/H_2O (2 mL/2 mL) solution (solution A). Separately, $(TBA)_2[W_6O_{19}]$ (11.5 μmol) and $(TBA)_4[\alpha\text{-SiW}_{12}O_{40}]$ (25.6 μmol) were added to the DMSO (2 mL) solution (solution B). To solution B, solution A was added, and the white-yellow crystalline solid **4** was successfully collected in almost quantitative yield (0.0910 g, 12.5 μmol, 98%). The addition of the excess amount of acetone to the filtrate gave a white-yellow crystal **2b** (0.0206 g, 6.40 μmol, 55% isolated yield).

Conclusion

The syntheses and characterizations of the Pd-based molecular triangle and square and hybrid composites with POMs were examined. The equilibrium between **1a** and **1b** largely depends on the solvents, and compounds **1a**,**b** were isolated in DMSO and water, respectively. The Pd-based molecular square-POM hybrid composites of **2a**,**b**, a mixture of **3a**,**b**, and **4** were synthesized by the reaction of **1a**/**1b** with $[W_6O_{19}]^{2-}$, $[W_{10}O_{32}]^{4-}$, and $[\alpha\text{-SiW}_{12}O_{40}]^{4-}$. The molecular square did not encapsulate the largest $[\alpha\text{-SiW}_{12}O_{40}]^{4-}$ in the cavity but did encapsulate $[W_6O_{19}]^{2-}$ and $[W_{10}O_{32}]^{4-}$. $[W_6O_{19}]^{2-}$ and $[\alpha\text{-SiW}_{12}O_{40}]^{4-}$ POMs could be isolated from the mixture by utilizing the quite different solubility of **2b** and **4** formed in DMSO. The size-selective encapsulation property of supramolecules may open a new way to rationalize the isolation methods of useful polyoxometalates. Catalyst design and the electrochemical study of supramolecule–polyoxometalate hybrid composites are in progress.

Acknowledgment. We acknowledge Prof. S. Hikichi (current address: Kanagawa University) for helpful discussions. This work was supported by the Core Research for Evolutional Science and Technology (CREST) program of the Japan Science and Technology Agency (JST) and a Grant-in-Aid for Scientific Research from the Ministry of Education, Culture, Science, Sports, and Technology of Japan.

Supporting Information Available: Selected spectroscopic data for **1a**,**b**, **2a**,**b**, **3a**,**b**, and **4** and the equilibrium between **1a** and **1b** at 294 K, ^{1}H NMR spectra in the region of 4,4′-bipyridine in DMSO-d_6 at 294 K, changes in the concentration of **1a**,**b** in D_2O at 298 K as a function of time, and numbering schemes of **1a**,**b**, **2a**,**b**, **3a**,**b**, and **4**. This material is available free of charge via the Internet at http://pubs.acs.org.

IC062156R